PCCP

COMMUNICATION

View Article Online
View Journal | View Issue

Cite this: *Phys. Chem. Chem. Phys.*, 2015, **17**, 24556

Received 12th June 2015,
Accepted 12th August 2015

DOI: 10.1039/c5cp03400k

www.rsc.org/pccp

Plasma induced tungsten doping of TiO_2 particles for enhancement of photocatalysis under visible light†

Yohei Ishida,[a] Yasutomo Motokane,[a] Tomoharu Tokunaga[b] and Tetsu Yonezawa*[a]

Here we report a novel method for modifying commercially available TiO_2 nanoparticles by a microwave-induced plasma technique. After the plasma treatment TiO_2 nanoparticles showed enhanced visible absorption due to the doped W atoms, and the photocatalytic methylene blue degradation above 440 nm was successfully improved.

Titanium dioxide (TiO_2) has attracted much attention across a wide field of research in recent decades due to its photocatalytic properties.[1,2] TiO_2 is a commercially available, cheap, and nontoxic photocatalyst that can decompose water or organic pollutants due to its excitation by sunlight. One limitation in current TiO_2 photocatalysis is its non-responsiveness under visible light. TiO_2 is a white powder and thus essentially has absorption below 387 nm (corresponding to 3.2 eV of the band-gap for anatase crystals[3]). To utilize a wide range of sunlight, visible-light responsive TiO_2 photocatalysts have been required. Recently, the modification of TiO_2 to obtain a visible-light responsive photocatalyst has become a major topic of research in the fields of photocatalysis,[1,4] green chemistry[1,4] and artificial photosynthesis.[5] Many modification strategies have been investigated, including the introduction of oxygen vacancies[6,7] and doping with heteroatoms such as Cr,[8] V,[8] N,[9] or S.[10]

The purpose of the current work is to present a novel strategy for modifying commercially available TiO_2 to obtain a visible-light responsive photocatalyst. Recently, a synthesis of metal nano-composites by using plasma in liquid has been developed. The radio wavelength region (usually 13.56 MHz) has been used as the main type of irradiation for producing plasma in the last decade,[11] but very recently the microwave region (2.45 GHz) has been introduced as a more readily available source.[12–15] Plasma is easily produced with relatively small microwave equipment owing to the high frequency of microwaves. During plasma production, bubbles continuously form and plasma is generated inside the bubbles or around the bubble boundary in the liquid, as reported in previous papers.[14,15]

We have recently reported the synthesis of Ag,[13] Pt,[13] and ZnO[12] nanoparticles by using microwave-induced plasma in an aqueous solution containing metal ions. The mechanism for the formation of metal nanoparticles is attributed to the reaction of metal ions with the $H^{\bullet}$ that results from the decomposition of water by plasma. With this background, we herein report a novel method for modifying TiO_2 nanoparticles by using microwave-induced plasma.

The modification of TiO_2 nanoparticles using microwave-induced plasma was carried out as described below. Among various types of TiO_2 nanoparticle, commercially available decahedral TiO_2 nanoparticles (Showa Denko Ceramics Co., Ltd., decahedral TiO_2[16]) were used because easy observation of the crystal phase by high-magnification scanning transmission electron microscopy (STEM) was expected.

A home-made microwave-induced liquid plasma system (see Fig. S1, ESI†) was used for the synthesis. 2 g of decahedral TiO_2 powder was dispersed in 500 mL deionized water (>18.2 MΩ, prepared by an Organo/ELGA purelabo system). Microwave plasma was introduced into this aqueous suspension at 400 W for various periods from 5 to 40 min under reduced pressure ($<2.1 \times 10^4$ Pa), using a diaphragm pump. After the plasma reaction, the resulting suspension was filtered using a membrane filter (ADVANTEC, 1.0 μm pore size) and dried overnight. Yellowish powder (see Fig. S2, ESI†) was obtained after 40 min plasma reaction.

The obtained TiO_2 powder was first characterized by XRD as shown in Fig. 1. Most importantly, characteristic peaks of TiO_2 were observed at 24–30 and 52–58 degrees. Bare decahedral TiO_2 shows sharp peaks of anatase crystal at 25.2, 37.3, 48.0, 53.7, 55.0, 62.5, 67.3, 70.0, 74.5, and 81.7 degrees, as well as relatively weak rutile peaks at 26.4 and 35.2 degrees. Since these peaks were also observed after plasma treatment for 5 to 40 min and did not change, it could be estimated that the crystal

[a] *Division of Material Science and Engineering, Faculty of Engineering, Hokkaido University, Kita 13 Nishi 8, Kita-ku, Sapporo, Hokkaido 060-8628, Japan. E-mail: tetsu@eng.hokudai.ac.jp*
[b] *Department of Quantum Engineering, Graduate School of Engineering, Nagoya University, Furo-cho, Chikusa-ku, Nagoya 464-8603, Aichi, Japan*

† Electronic supplementary information (ESI) available: Detailed experimental procedures. See DOI: 10.1039/c5cp03400k

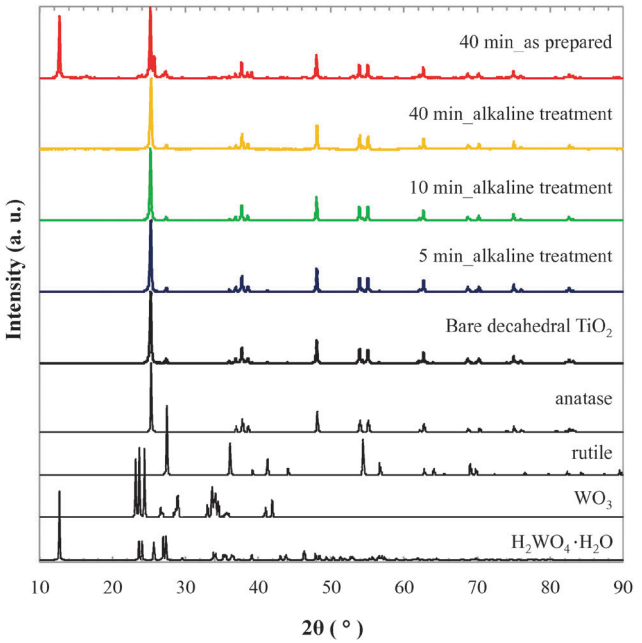

Fig. 1 XRD patterns of plasma-modified decahedral TiO_2 nanoparticles. References were obtained from JCPDS data: anatase (00-021-1272), rutile (00-021-1276), WO_3 (00-032-1395), and $H_2WO_4{\cdot}H_2O$ (00-018-1420).

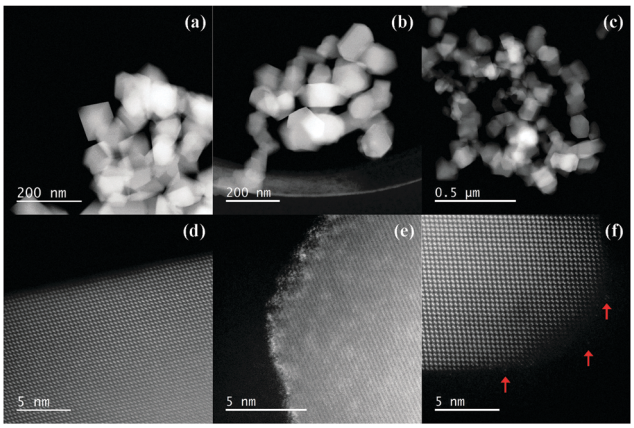

Fig. 2 HAADF-STEM images of decahedral bare TiO_2 powder (a and d), and the TiO_2 following 40 min plasma reaction before (b and e) and after (c and f) alkaline treatment.

structure was maintained even during the plasma treatment. After 40 min of plasma treatment (red line in Fig. 1), small patterns corresponding to tungsten components were detected at 23.2, 26.2, around 35, and 40.2 degrees (WO_3) and at 10.5, 42.5, and 45.2 degrees ($H_2WO_4{\cdot}H_2O$). These W components were contaminants from the electrode used in the plasma equipment (see Fig. S1, ESI†). In fact, the surface of the W electrode was slightly damaged after plasma irradiation. To obtain pure Ti components and accurately investigate their characteristics, we endeavoured to remove the W components using alkaline solution. Tungsten oxides can be readily dissolved in aqueous alkali. It is known that nano W components are easily oxidized, and the resulting oxides can dissolve in concentrated NaOH aqueous solution.[17] We introduced 300 mL of NaOH solution (*ca.* pH 13) to 1.0 g of the resulting TiO_2 powder and stirred the mixture for 30 min. It was then filtered and repeatedly washed with deionized water. The XRD patterns of the W components disappeared completely after the alkaline treatment (yellow line), thus we succeeded in the purification of plasma-modified TiO_2 powder. The yellowish color of the as-prepared TiO_2 nanoparticles (plasma for 40 min) turned to light ash (see Fig. S2, ESI†) after the alkaline treatment. This color change is attributed to the removal of yellowish WO_3 and $H_2WO_4{\cdot}H_2O$, which usually have absorption below 500[18] and 520[18] nm, respectively. All samples were successfully purified by the same procedure. Their XRD patterns are summarized in Fig. 1.

Fig. 2a–c show high-angle annular dark-field scanning transmission electron microscopic (HAADF-STEM) images of bare decahedral TiO_2 (a), and the TiO_2 following plasma reaction for 40 min before (b) and after (c) alkaline treatment. Particles around 50 to 250 nm in diameter with decahedral structures were observed in these 3 images, as reported in a previous paper.[16] From these HAADF-STEM images, we can conclude that the particle size and shape of the TiO_2 did not change during the plasma and alkaline treatments.

High-magnification HAADF-STEM images are shown in Fig. 2d–f. The HAADF-STEM method enables the observation of chemical contrast according to the atomic number (Z). In the present case, the atomic number of ^{22}Ti is much smaller than that of ^{74}W, thus the contaminating W components can be detected. The bare decahedral TiO_2 nanoparticle has a flat surface with atomic precision (Fig. 2d). After the plasma treatment, the surface became rough (sometimes called a "damaged surface") and the contrast on the surface is much higher than that in the inner region (Fig. 2e). The rough surface is a result of the extremely high temperature of plasma (several thousand °C). Since the melting point of TiO_2 is *ca.* 1840 °C,[19] the current experimental temperature may melt the surface of the TiO_2 particles. After the alkaline treatment, we did not observe any high-contrast surfaces (Fig. 2f), and the rough surface remained. The absence of the high-contrast layer is attributed to the removal of W components on the particle surface by the alkaline treatment. However, even after the alkaline treatment we still observed bright spots in the particle region, as indicated by the red arrows in Fig. 2f. These spots must be composed of heavier atoms than the background (Ti and O), thus they are estimated to be the doped W atoms introduced from the electrode in the plasma equipment.

In order to determine the loading amount of W atoms in the TiO_2 nanoparticles, inductively coupled plasma atomic emission spectroscopy (ICP-AES) was carried out (see the experimental procedure in ESI†). As a result, the atomic percent of W (= W/Ti × 100%) was determined to be 0.0, 0.1, 0.2, and 0.2% for 0 (bare), 5, 10, and 40 min samples, respectively. The loading amount seemed to be saturated after 10 min of plasma treatment. This phenomenon will be discussed in the diffuse reflectance spectra (Fig. 3). STEM energy-dispersive X-ray spectroscopy (EDX) analysis was also carried out (Fig. S3, ESI†). The plasma-treated decahedral TiO_2 particles clearly showed W components on their surfaces (before the alkaline treatment, Fig. S3a, ESI†). On the other

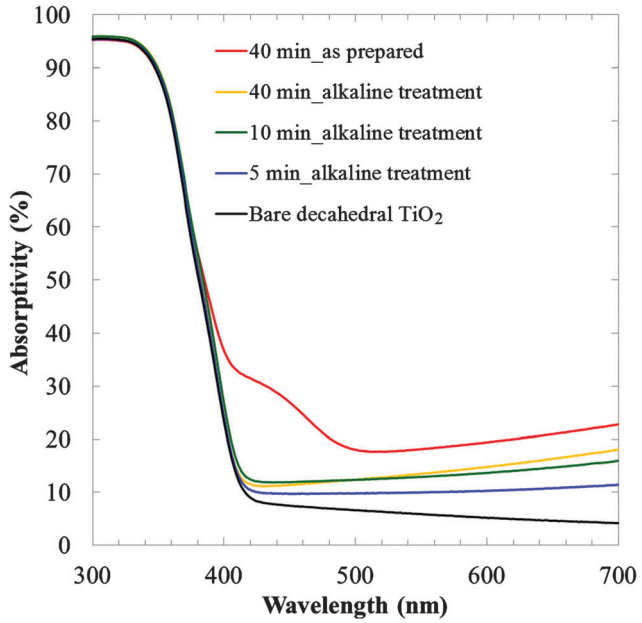

Fig. 3 UV-Vis diffuse reflectance spectra of decahedral TiO_2 nanoparticles.

hand, the surface W components were eliminated after the alkaline treatment (Fig. S3b, ESI†). These observations strongly support the discussions of the XRD (Fig. 1) and STEM (Fig. 2) results. It should be noted that we still observed weak, but strong enough W components even after the alkaline treatment. The counts of W mapping were rather stronger than the background. Therefore we concluded that W atoms were doped inside the TiO_2 crystal structure from the electrode in the plasma equipment, as discussed for Fig. 2f and the ICP-AES. The ionic radii of Ti and W are 60.5 and 60.0 pm,[20] respectively, thus the W atom should be able to substitute for Ti in the crystal structure. The ICP-AES and STEM-EDX results clearly indicate that the microwave-induced plasma technique can dope W atoms into TiO_2 nanoparticles.

The photocatalytic performance of our plasma-modified decahedral TiO_2 nanoparticles was investigated. First, the diffuse reflectance spectra were recorded for 300–800 nm with a baseline corresponding to $BaSO_4$, as shown in Fig. 3 (see also the spectra for 300–2000 nm in Fig. S4, ESI†). The bare decahedral TiO_2 does not have visible light reflectance over 400 nm (black line). On the other hand, visible light reflectance was obtained after the plasma treatment. This reflectance enhancement is probably derived from the doping of W atoms as observed in Fig. 2. It is known that the conduction band of TiO_2 gradually moves downward with increasing W loading amount below 2%, which results in the red shift of absorption.[21] The as-prepared plasma-treated TiO_2 (40 min, red line) showed characteristic absorption around 400–500 nm, which disappeared after the alkaline treatment (yellow line). It is known that WO_3 and $H_2WO_4{\cdot}H_2O$ have characteristic absorption at 500 and 520 nm,[18] respectively. Thus, the diffuse reflectance spectra also support the successful removal of W components. The visible light reflectance of the 10 and 40 min samples was almost the same. This result suggests that the effect of plasma on the absorption enhancement of decahedral TiO_2 nanoparticles was saturated. This result is in agreement with the loading amount of W determined by ICP-AES. Judging from the reflectance, *ca.* 12% enhancement of the reflectance at 600 nm for bare TiO_2 is the saturation point of the current plasma treatment (5 min was not saturated, as can be seen from the blue line). A plausible reason for the saturation is the large particle diameter of the decahedral TiO_2 nanoparticles (50–250 nm[16]). Such large particles have relatively small specific surface areas and the total rate for modification of the surface regions is limited. Our preliminary experiment using similar liquid plasma for smaller TiO_2 nanoparticles (ISK, ST-01, *ca.* 5 nm particle diameter determined by TEM) showed a much more drastic enhancement in their visible-light reflectance (not shown). These results will be reported soon. Synthesis of visible-light responsive TiO_2 nanoparticles is attracting much attention for future photocatalysis utilizing wide wavelength regions of sunlight. Our liquid plasma method will thus widen the spectrum of modification strategies for obtaining functionalized TiO_2 nanoparticles.

A preliminary investigation of the photocatalytic performance of our decahedral TiO_2 nanoparticles was carried out by the methylene blue (MB) degradation test under visible-light irradiation.[2] A Hg–Xe lamp (San-ei electric, UVF-204S, 200 W) was used as an excitation light source with an optical cut filter for <440 nm. The experimental procedure was as follows. 50 mg of TiO_2 powder was dispersed in 40 mL of 10 mg L^{-1} MB aqueous solution. The mixture was stirred for 30 min in the dark. 1 mL of the sample was taken and centrifuged at 6300 rpm for 3 min to precipitate the TiO_2 powder. The supernatant was put into a quartz cell with a 1 mm optical path, and we measured the absorption spectrum (Shimadzu, UV-1800) in order to determine the initial concentration of MB. Irradiation was then commenced, and we measured the absorption spectrum of the supernatant every 30 min.

The degradation of MB could be analyzed by first-order kinetics with the classical equation $\ln(C_0/C) = kt$, where C_0 and C indicate the absorbance at 665 nm before and after irradiation, respectively, k is the rate constant, and t is the irradiation time. Fig. 4 shows the concentration change of MB, $\ln(C_0/C)$, as a function of irradiation time. Fig. S5 in the ESI† shows the raw absorption spectral change during the excitation. As can be seen from Fig. 4, it is clear that the plasma-treated TiO_2 showed better performance than that of the bare decahedral TiO_2. The reaction rate constants (k) of bare, 10 and 40 min plasma-treated TiO_2 were 2.3×10^3, 2.6×10^3 and 2.8×10^3 min^{-1}, respectively. From these values, it is expected that a longer plasma time results in better photocatalytic performance under visible light. The photocatalytic enhancement was not derived from the specific surface area (the particle size and shape remained the same, as shown in Fig. 2); the enhanced visible-light reflectance is the main reason. We conclude that the liquid plasma technique enables visible-light responsive photocatalysis in an easy and simple manner. Although the loading amount of W in the TiO_2 nanoparticles

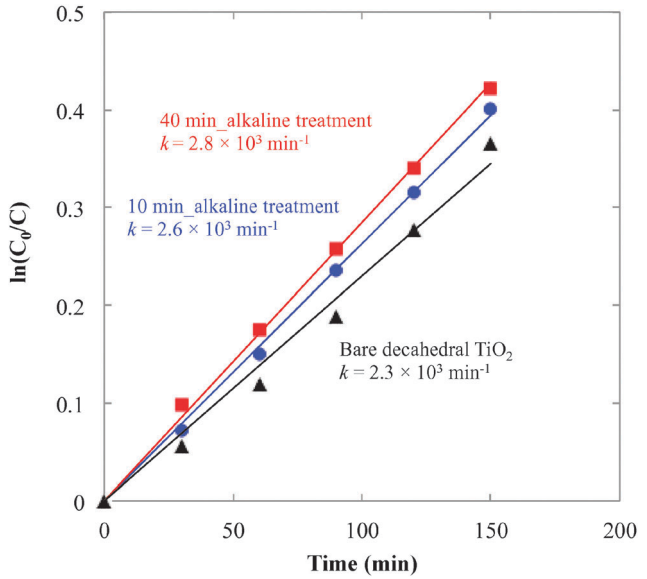

Fig. 4 MB degradation under irradiation above 440 nm. C_0 and C indicate the absorbance at 665 nm before and after irradiation, respectively. k indicates the photocatalysis reaction rate constant.

and the photocatalytic performance were almost saturated after 10 min (from the ICP and UV-Vis results), a larger specific surface area of TiO_2 nanoparticles or stronger plasma power may result in a larger amount of W doping in the nanoparticles.

In conclusion, we have presented a novel procedure for modifying commercially available decahedral TiO_2 nanoparticles by using microwave-induced plasma. The size and shape of decahedral TiO_2 did not change during the plasma treatment. A damaged surface layer was observed after the plasma treatment, and moreover, the doping of W atoms in the TiO_2 structure was deduced from the high-magnification HAADF-STEM and EDX mapping. The photocatalytic methylene blue degradation under irradiation above 440 nm was successfully improved, which was attributed to the enhancement of visible-light reflectance. The simple and easy procedure presented here will therefore widen the range of modification strategies to obtain functionalized TiO_2 photocatalysts.

Experimental section

The microwave generator was a UW-1500 (Micro-Denshi, Japan) at 2.45 GHz. Microwaves were emitted from the magnetron passing through a WRJ-2 rectangular wave guide (109.22 × 54.61 mm), a power meter, a tuner, and a waveguide to the coaxial adaptor. The electrodes were made of tungsten (experimental setup illustrated in Fig. S1, ESI†). For characterization, XRD (Rigaku, MiniFlexII), STEM-HAADF (JEOL, JEM-ARM200, acceleration voltage of 200 kV), STEM-EDX (FEI, TITAN III G2 Cubed, 300 kV) and diffuse reflectance spectroscopy (JASCO, V-670) were used. ICP-AES was measured with a Thermo SCIENTIFIC iCAP 6000.

Acknowledgements

This work was partly supported by a Research Fund from Hokkaido University to YI and TY, and by a Grant-in-Aid for Scientific Research (A) from JSPS (24241041). This work was also partially supported by Hokkaido University, microstructural characterization platform as a program of Nanotechnology Platform of the Ministry of Education, Culture, Sports, Science and Technology (MEXT), Japan. The authors thank Prof. B. Ohtani (Hokkaido Univ.) for fruitful discussion. A part of this work was also supported by the Advanced Characterization Nanotechnology Platform of the National Institute for Materials Science and the High Voltage Electron Microscopy Laboratory of Nagoya University.

Notes and references

1 A. Fujishima and K. Honda, *Nature*, 1972, **238**, 37.
2 C. Xue, T. Narushima, Y. Ishida, T. Tokunaga and T. Yonezawa, *ACS Appl. Mater. Interfaces*, 2014, **6**, 19924.
3 H. Tang, K. Prasad, R. Sanjines, P. E. Schmid and F. Levy, *J. Appl. Phys.*, 1994, **75**, 2042.
4 A. Fujishima, T. N. Rao and D. A. Tryk, *J. Photochem. Photobiol., C*, 2000, **1**, 1.
5 S. Okunaka, H. Tokudome, Y. Hitomi and R. Abe, *J. Mater. Chem. A*, 2015, **3**, 1688.
6 X. Chen, L. Liu, P. Y. Yu and S. S. Mao, *Science*, 2011, **331**, 746.
7 I. Nakamura, N. Negishi, S. Kutsuna, T. Ihara, S. Sugihara and K. Takeuchi, *J. Mol. Catal. A: Chem.*, 2000, **161**, 205.
8 M. Anpo and M. Takeuchi, *Int. J. Photoenergy*, 2001, **3**, 89.
9 R. Asahi, T. Morikawa, T. Ohwaki, K. Aoki and Y. Taga, *Science*, 2001, **293**, 269.
10 T. Umebayashi, T. Yamaki, H. Itoh and K. Asai, *Appl. Phys. Lett.*, 2002, **81**, 454.
11 T. Ihara, M. Miyoshi, M. Ando, S. Sugihara and Y. Iriyama, *J. Mater. Sci.*, 2001, **36**, 4201.
12 T. Yonezawa, A. Hyono, S. Sato and O. Ariyada, *Chem. Lett.*, 2010, **39**, 783.
13 S. Sato, K. Mori, O. Ariyada, A. Hyono and T. Yonezawa, *Surf. Coat. Technol.*, 2011, **206**, 955.
14 S. Nomura, H. Toyota, M. Tawara, H. Yamashita and K. Matsumoto, *Appl. Phys. Lett.*, 2006, **88**, 231502.
15 S. Nomura, *J. Plasma Fusion Res.*, 2013, **89**, 199.
16 F. Amano, O. O. P. Mahaney, Y. Terada, T. Yasumoto, T. Shibayama and B. Ohtani, *Chem. Mater.*, 2009, **21**, 2601.
17 R. Jedamzik, A. Neubrand and J. Rödel, *J. Mater. Sci.*, 2000, **35**, 477.
18 J. Cao, B. Luo, H. Lin, B. Xu and S. Chen, *Appl. Catal., B*, 2012, **111**, 288.
19 J. Hlavac, *Pure Appl. Chem.*, 1982, **54**, 681.
20 R. D. Shannon, *Acta Crystallogr., Sect. A: Cryst. Phys., Diffr., Theor. Gen. Crystallogr.*, 1976, **32**, 751.
21 Z. Xi, L. Fang, H. L. Qiu, Z. Gang and W. S. Zhong, *J. Phys. Chem. C*, 2011, **115**, 12665.